STRUCTURES FOR TIME-REVERSED INVERSION IN FILTER BANKS

P. P. Vaidyanathan[1] and Tsuhan Chen[2]

[1]Dept. Electrical Engr., Caltech, Pasadena, CA 91125
[2]AT&T Bell Laboratories, Holmdel, NJ 07733-3030

Abstract

Anticausal inversion of IIR transfer functions has gained importance in recent years, in the efficient implementation of IIR digital filter banks. In this paper we first introduce the idea of a causal dual, as an intermediate step in the implementation of anticausal IIR inverses. With time reversal operators at the input and output of the casusal dual, we get the anticausal inverse of the original structure. The causal dual eliminates the need for similarity transformations, during a key step called *blockwise state transfer,* in implementing anticausal inverses. In the paper we identify efficient structures for causal duals of standard structures like the direct-form, cascade-form, coupled form, and IIR lattice structures, including the tapped lattice.

1. INTRODUCTION

Anticausal inversion of IIR transfer functions has gained importance in recent years, in the implementation of digital filter banks [1]–[6]. This is due to a certain class of IIR digital filter banks, in which the synthesis filters are required to be anticausal if a stable reconstruction system (synthesis bank) is desired. Thus, Fig. 1.1 shows the polyphase form [7] of a commonly used two channel filter bank. This has perfect reconstruction $[\widehat{x}(n) = x(n)]$ if and only if $R_i(z) = 1/E_i(z)$. If $E_i(z)$ does not have all zeros inside the unit circle, then the causal impulse response of $R_i(z)$ is unstable. In some cases (e.g., when $E_i(z)$ is allpass with poles inside the unit circle), $1/E_i(z)$ has all poles outside, so that an anticausal impulse response of $1/E_i(z)$ is stable. This explains the interest in implementing anticausal inverses. This has been shown to be possible [3]-[6], even in real time with infinite duration inputs, as long as we perform the processing in blocks of length L, and properly transmit the state variables from $E_i(z)$ to $1/E_i(z)$ at the end of each block.

Consider a causal stable Nth order filter $G(z)$, implemented using a minimal structure (direct-form, lattice, etc.), with state space description

$$\begin{bmatrix} \mathbf{x}(n+1) \\ y(n) \end{bmatrix} = \underbrace{\begin{bmatrix} \mathbf{A} & \mathbf{B} \\ \mathbf{C} & D \end{bmatrix}}_{\mathcal{R}} \begin{bmatrix} \mathbf{x}(n) \\ u(n) \end{bmatrix} \qquad (1.1)$$

Work supported in parts by the Office of Naval Research grant N00014-93-1-0231, Rockwell Intl., and Tektronix, Inc.

where $\mathbf{x}(n) = [x_1(n) \quad \dots \quad x_N(n)]^T$ is the state vector $[x_i(n)$ are the outputs of delays], $u(n)$ is the filter input and $y(n)$ the filter output. The transfer function is given by $G(z) = D + \mathbf{C}(z\mathbf{I} - \mathbf{A})^{-1}\mathbf{B}$ and has an anticausal inverse [i.e., there is an anticausal inverse z-transform of $1/G(z)$] if and only if the *realization matrix* $\mathcal{R}$ is nonsingular [5]. We assume this. Consider the following "dual" casual state space equations

$$\begin{bmatrix} \widehat{\mathbf{x}}(n+1) \\ \widehat{y}(n) \end{bmatrix} = \underbrace{\begin{bmatrix} \widehat{\mathbf{A}} & \widehat{\mathbf{B}} \\ \widehat{\mathbf{C}} & \widehat{D} \end{bmatrix}}_{\widehat{\mathcal{R}}} \begin{bmatrix} \widehat{\mathbf{x}}(n) \\ \widehat{u}(n) \end{bmatrix} \qquad (1.2)$$

where $\widehat{\mathcal{R}} = \mathcal{R}^{-1}$. Imagine we run the original system (1.1) for a duration of L samples, with input $u(0) \dots u(L-1)$ and get the output $y(0) \dots y(L-1)$ and final state $\mathbf{x}(L)$. If we run the state space equations (1.2) by setting the initial state to be $\widehat{\mathbf{x}}(L) = \mathbf{x}(L)$, and the input sequence to be the time reversed block $y(L-1) \dots y(0)$, we can show that the output of this system for the duration of this block is $u(L-1) \dots u(0)$. In this way we can invert (1.1), i.e., invert $G(z)$. Since the time reversal is blockwise, it can be realized in practice with finite latency. By repeating the above process block by block, we can implement the anticausal inverse $1/G(z)$ of the original filter $G(z)$, even for infinitely long inputs.

It can be shown that the transfer function of the causal system (1.2) is $1/G(z^{-1})$. We can schematically express the desired anticausal inverse $1/G(z)$ as in Fig. 1.2, in terms of ideal time reversal (TR) operators. In a practical implementation of the "anticausal" inverse $1/G(z)$, the time reversals are done blockwise, and the causal system $1/G(z^{-1})$ implemented using (1.2). The initial condition for the state recursion (1.2) at the beginning of each block is taken as the final state from the previous block of the state recursion (1.1) for $G(z)$. This **state transfer** is crucial.

Aim of the Paper

Note that $1/G(z^{-1})$ can be realized using any structure (direct-form, lattice, etc.). The state space description of these structures are related to $(\widehat{\mathbf{A}}, \widehat{\mathbf{B}}, \widehat{\mathbf{C}}, \widehat{D})$ by similarity transforms. If an arbitrary structure is used for $1/G(z^{-1})$, then the *state transfer* described above should be done only after a similarity transformation at the beginning of each block.

Causal dual of a structure. A structure for $1/G(z^{-1})$ which has precisely the state space description $(\widehat{\mathbf{A}}, \widehat{\mathbf{B}}, \widehat{\mathbf{C}}, \widehat{D})$ will be called a *causal dual* of the structure $(\mathbf{A}, \mathbf{B}, \mathbf{C}, D)$ for $G(z)$. If the causal dual is used for implementing $1/G(z^{-1})$, no similarity transformations are necessary during state transfer. *In this paper we will identify efficient structures for the causal duals of standard structures,* such as the direct-form, cascade-form, coupled form, and the family of lattice structures, including the tapped lattice.

2. CAUSAL DUAL FOR THE DIRECT-FORM

Fig. 2.1(a) shows the direct form for an Nth order filter $G(z)$. From [5] we know that the inverse filter $1/G(z)$ has an anticausal impulse response (more simply, $G(z)$ has an anticausal inverse) if and only if $p_N \neq 0$; we therefore assume this. With the state variables $x_i(n)$ as indicated in the figure, the matrix $\mathbf{A}$ is in companion form (e.g., see [7]). Writing down the realization matrix $\mathcal{R}$, we can explicitly invert it, and verify that the structure in Fig. 2.1(b) has the realization matrix $\mathcal{R}^{-1}$, and is therefore the causal dual. Thus the causal dual can be obtained by making a simple set of changes to the multipliers, and renumbering the state variables in reverse order. For the special case of allpass filters the causal dual is even simpler, since $p_n = q^*_{N-n}$. For real coefficient allpass filters, *the direct form structure is its own causal causal dual* — only the states need to be renumbered. This is consistent with the anticausal inversion of direct-form reported in [8].

Cascade-form structures. The cascade-form, which is a cascade connection of second order direct form structures, is well-known for its simplicity and relatively better robustness to quantization [10]. More generally, let $G_1(z)$ and $G_2(z)$ be causal transfer functions in cascade (Fig. 2.2), implemented with structures having realization matrices $\mathcal{R}_1$ and $\mathcal{R}_2$. Then from the block of L outputs $y_2(n) \ldots y_2(n+L-1)$ and the state $\mathbf{x}_2(n+L)$ of $G_2(z)$, we can recover the block of L inputs $y_1(n) \ldots y_1(n+L-1)$ of the system $G_2(z)$. We can then use $y_1(n) \ldots y_1(n+L-1)$ (output block of $G_1(z)$) and the state vector $\mathbf{x}_1(n+L)$ of the system $G_1(z)$ to recover the primary input block $u(n) \ldots u(n+L-1)$. This is equivalent to connecting the anticausal inverses in *reverse order.*

In fact, it can be shown that the causal dual of a cascade is simply the cascade of the individual causal duals, in reverse order. If we implement this cascaded causal dual structure with blockwise time reversal of its primary input and output, we obtain the anticausal implementation of the complete system $1/G(z)$. Thus, regardless of the number of filters connected in cascade, time reversal is necessary only at the primary input and output nodes, and not at the intermediate inputs and outputs.

3. CAUSAL DUAL FOR THE COUPLED-FORM

Fig. 3.1(a) shows the coupled form structure, whose robustness to quantization is well-known [10]. The poles of this system are at $\rho e^{j\theta}$ and $\rho e^{-j\theta}$. With the output node $y(n)$ as indicated, the transfer function is $G(z) = \rho \sin\theta z^{-2}/(1 - 2\rho\cos\theta z^{-1} + \rho^2 z^{-2})$. Upon analysis we find that the realization matrix is

$$\mathcal{R}_{couple} = \begin{bmatrix} \mathbf{A} & \mathbf{B} \\ \mathbf{C} & D \end{bmatrix} = \begin{bmatrix} \rho\cos\theta & -\rho\sin\theta & 1 \\ \rho\sin\theta & \rho\cos\theta & 0 \\ 0 & 1 & 0 \end{bmatrix}$$

The inverse of this matrix is

$$\mathcal{R}^{-1}_{couple} = \begin{bmatrix} 0 & 1/\rho\sin\theta & -\cot\theta \\ 0 & 0 & 1 \\ 1 & -\cot\theta & \rho\sin\theta + \rho\cot\theta\cos\theta \end{bmatrix}$$

Fig. 3.1(b) shows the structure with this realization matrix (where $m = \rho\sin\theta + \rho\cot\theta\cos\theta$). This is the causal dual of Fig. 3.1(a). Note that $\widehat{\mathbf{A}}$ (the top-left 2×2 matrix above) has all eigenvalues $= 0$. This is because $1/G(z^{-1})$ is FIR.

The Tapped Coupled Form. Fig. 3.2(a) shows the tapped coupled form. This has the extra multipliers (tap coefficients) D, c_1 and c_2 which can be used to obtain arbitrary numerators. The realization matrix now becomes

$$\mathcal{R}_{tap} = \begin{bmatrix} \rho\cos\theta & -\rho\sin\theta & 1 \\ \rho\sin\theta & \rho\cos\theta & 0 \\ c_1 & c_2 & D \end{bmatrix} \qquad (3.1)$$

which can be rewritten as

$$\mathcal{R}_{tap} = \begin{bmatrix} 1 & 0 & 0 \\ 0 & 1 & 0 \\ D & \alpha & \beta \end{bmatrix} \underbrace{\begin{bmatrix} \rho\cos\theta & -\rho\sin\theta & 1 \\ \rho\sin\theta & \rho\cos\theta & 0 \\ 0 & 1 & 0 \end{bmatrix}}_{\mathcal{R}_{couple}} \qquad (3.2)$$

with $\alpha = (c_1 - D\rho\cos\theta)/\rho\sin\theta$, $\beta = c_2 + D\rho\sin\theta - \alpha\rho\cos\theta$. Thus $\mathcal{R}^{-1}_{tap}$ can be written as

$$\mathcal{R}^{-1}_{tap} = \mathcal{R}^{-1}_{couple} \begin{bmatrix} 1 & 0 & 0 \\ 0 & 1 & 0 \\ -D/\beta & -\alpha/\beta & 1/\beta \end{bmatrix} \qquad (3.3)$$

The structure with this realization matrix can be obtained from Fig. 3.1(b) by replacing the input $\widehat{u}(n)$ with $-(D/\beta)\widehat{x}_1(n) - (\alpha/\beta)\widehat{x}_2(n) + (1/\beta)\widehat{u}(n)$, as shown in Fig. 3.2(b). This is therefore the causal dual of the tapped coupled-form.

4. CAUSAL DUALS FOR LATTICE STRUCTURES

In the case of the direct form structure, we could obtain the causal dual simply by inspection (Fig. 2.1). For arbitrary structures, the rules could be more complicated, as shown by the coupled form example. We will see next that for the lattice structures, which are well-known for many good robustness properties [11]–[12], the causal dual can be obtained again by inspection! The lattice structure is shown in Fig. 4.1(a). Here $G_N(z) = Y(z)/U(z)$ is a causal Nth order allpass filter. The rectangular building block labelled k_m can take

several possible forms (Fig. 4.1(b)). While the normalized structure offers automatic scaling and normalization of noise gains [11], the two-multiplier version offers economy. For a given set of lattice coefficietns $\{k_m\}$, the allpass function $G_N(z)$ is the same regardless of which of these building blocks is used. The lattice coefficients k_m are possibly complex, but $|k_m| < 1$, so $G_N(z)$ is stable. The multiplier $\widehat{k}_m = \sqrt{1-|k_m|^2}$ is always real.

With the state variables $x_m(n)$, the input $u(n)$ and output $y(n)$ indicated as shown in Fig. 4.1(a), let the realization matrix of this Nth order structure be denoted as $\mathcal{R}_N$. We will show that the causal dual (i.e., the structure with realization matrix $\mathcal{R}_N^{-1}$) is as shown in Fig. 4.2, where the boxes k_m^* are the builing blocks in the original structure Fig. 4.1, but with coefficients conjugated. Thus the causal dual structure is obtained from the original structure by *conjugating the multipliers, and moving the delays from the bottom rails to the top rails.*

For Fig. 4.2, define the state vector $\widehat{\mathbf{x}}(n)$ and the state space description $(\widehat{\mathbf{A}}, \widehat{\mathbf{B}}, \widehat{\mathbf{C}}, \widehat{D})$, and let the realization matrix be denoted $\widehat{\mathcal{R}}_N$. First consider the normalized lattice. In this case $\mathcal{R}_N$ is unitary [13], so we only have to show $\widehat{\mathcal{R}}_N = \mathcal{R}_N^\dagger$ (transpose conjugate). This is based on:

Lemma 3.1. The $(N+1) \times (N+1)$ realization matrix $\mathcal{R}_N$ for the lattice of Fig. 4.1(a) with normalized building blocks can be expressed as a product of N unitary matrices:

$$\begin{bmatrix} \Theta_1 & 0 \\ 0 & \mathbf{I}_{N-1} \end{bmatrix} \begin{bmatrix} 1 & 0 & 0 \\ 0 & \Theta_2 & 0 \\ 0 & 0 & \mathbf{I}_{N-2} \end{bmatrix} \cdots \begin{bmatrix} \mathbf{I}_{N-1} & 0 \\ 0 & \Theta_N \end{bmatrix}$$

where the unitary matrix $\Theta_m \triangleq \begin{bmatrix} -k_m & \widehat{k}_m \\ \widehat{k}_m & k_m^* \end{bmatrix}$. ◇

Proof. It can be shown that realization matrix of the m-stage lattice and the $(m-1)$-stage lattice are related as

$$\mathcal{R}_m = \begin{bmatrix} \mathcal{R}_{m-1} & 0 \\ 0 & 1 \end{bmatrix} \begin{bmatrix} \mathbf{I} & 0 \\ 0 & \Theta_m \end{bmatrix} \qquad (4.1)$$

For $m = 1$ we can explicitly verify that $\mathcal{R}_1 = \Theta_1$. The lemma follows from this by induction. ▽▽▽

Theorem 3.1. Causal dual for normalized lattice. The causal dual of the normalized lattice structure (Fig. 4.1(a), with normalized building blocks) is given by the lattice of Fig. 4.2. ◇

Proof. We can show that the realization matrices for the m-stage lattice and $(m-1)$-stage lattice in Fig. 4.2 are related as

$$\widehat{\mathcal{R}}_m = \begin{bmatrix} \mathbf{I} & 0 \\ 0 & \Theta_m^\dagger \end{bmatrix} \begin{bmatrix} \widehat{\mathcal{R}}_{m-1} & 0 \\ 0 & 1 \end{bmatrix} \qquad (4.2)$$

and we can explicitly verify that $\widehat{\mathcal{R}}_1 = \Theta_1^\dagger$. From these we can obtain $\widehat{\mathcal{R}}_N = \mathcal{R}_N^\dagger = \mathcal{R}_N^{-1}$. ▽▽▽

Real coefficient case. If $G_N(z)$ has real coefficients, then k_m are real. So the causal dual is identical to the original structure, except that delays have to be moved up.

Denormalized lattice sections. Suppose the lattice structure of Fig. 4.1(a) uses denormalized sections (e.g., the two multiplier section of Fig. 4.1(b), or one-multiplier sections which are available for real coefficient case [7]). Then the structure is related to the normalized lattice via a diagonal similarity transformation. Using this, it is possible to show that if Fig. 4.1(a) represents a denormalized lattice, then Fig. 4.2 still represents its causal dual. That is, we simply conjugate coefficients and move the delays to upper rails.

The Tapped Lattice Structure. The tapped lattice, which can be used to realize an arbitrary IIR transfer function $H(z)$ is shown in Fig. 4.3(a). Here $H(z)$ has denominator equal to the that of the allpass filter $G_N(z)$. The tap coefficients α_n can be chosen to realize the numerator of $H(z)$. We will show that the causal dual of this is given by Fig. 4.3(b). (This assumes $\alpha_{N+1} \neq 0$. If $\alpha_{N+1} = 0$, the numerator of $H(z)$ has a smaller order than the denominator, and an anticausal inverse does not exist [5]. The causal dual would then be of no interest.)

For fixed input $u(n)$, the state variables $x_i(n)$ in Figs. 4.3(a) and 4.1(a) are identical. In Fig. 4.3(a) $y_1(n) = \sum_{i=1}^N \alpha_i x_i(n+1) + \alpha_{N+1} y(n)$. Thus the realization matrix $\mathcal{R}_{arb}$ for the arbitrary transfer function $H(z)$ is related to the realization matrix $\mathcal{R}_{all}$ of the allpass filter $G_N(z)$ as

$$\mathcal{R}_{arb} = \begin{bmatrix} \mathbf{I} & 0 \\ \mathbf{a} & \alpha_{N+1} \end{bmatrix} \mathcal{R}_{all} \qquad (4.3)$$

where $\mathbf{a} = [\alpha_1 \quad \alpha_2 \quad \ldots \quad \alpha_N]$. Thus

$$\mathcal{R}_{arb}^{-1} = \mathcal{R}_{all}^{-1} \begin{bmatrix} \mathbf{I} & 0 \\ -\mathbf{a}/\alpha_{N+1} & 1/\alpha_{N+1} \end{bmatrix} \qquad (4.4)$$

Since $\mathcal{R}_{all}^{-1}$ corresponds to Fig. 4.2, the above realization matrix corresponds to the structure Fig. 4.3(b), which is therefore the causal dual of Fig. 4.3(a). This has taps in a feedback loop. Whether this is stable depends on the numerator of $H(z)$.

References

[1] Ramstad, T. A. "IIR filterbank for subband coding of images," Proc. of the IEEE ISCAS, pp. 827-830, Finland, June 1988.

[2] Husoy, J., and Ramstad, T. A. "Application of an efficient parallel IIR filter bank to image subband coding," *Signal Processing,* August 1990, pp. 279–292.

[3] Babic, H., Mitra, S. K., Creusere, C. D., and Das, A., "Perfect reconstruction recursive QMF banks for image subband coding," Proc. 25th Annual Asil. Conf. Sig., Sys. and Comp., Nov. 1991.

[4] Mitra, S. K., Creusere, C. D., and Babic, H. "A novel implementation of perfect reconstruction QMF banks using IIR filters for infinite length signals," Proc. IEEE ISCAS, pp. 2312–2315, San Diego, May 1992.

A-1

[5] Vaidyanathan, P. P., and Chen, T. "Role of anticausal inverses in multirate filter-banks – Part I: System-Theoretic Fundamentals, and Part II: The FIR Case, Factorizations, and biorthogonal Lapped Transforms," IEEE Trans. SP (submitted).

[6] Chen, T., and Vaidyanathan, P. P. "General theory of time-reversed inversion for perfect reconstruction filter banks," Proc. 26th Annual Asilomar Conf. Sig., Sys. and Comp., pp. 821–825, Oct. 1992.

[7] Vaidyanathan, P. P. *Multirate systems and filter banks,* Prentice Hall, 1993.

[8] Creusere, C. D. *PR Modulated polyphase filter banks using time-reversed subfilters,* Ph.D Dissertation, Dept. ECE, UCSB, 1993.

[9] Vaidyanathan, P. P., and Chen, T. "Structures for anticausal inverses in multirate filter banks," in preparation.

[10] Oppenheim, A. V., and Schafer, R. W. *Discrete-time signal processing,* Prentice Hall, Inc., 1989.

[11] Gray, Jr., A. H., and Markel, J. D. "A normalized digital filter structure," *IEEE Trans. ASSP,* pp. 268-277, June 1975.

[12] Gray, Jr., A. H. "Passive cascaded lattice digital filters," *IEEE Trans. CAS,* pp. 337-344, May 1980.

[13] Vaidyanathan, P. P. "The discrete-time bounded real lemma in digital filtering," IEEE Trans. CAS, pp. 918–924, Sept. 1985.

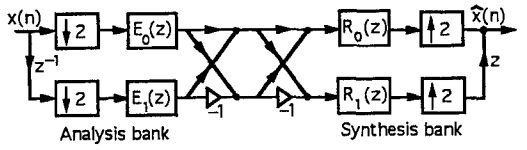

Fig. 1.1. A two-channel filter bank in polyphase form.

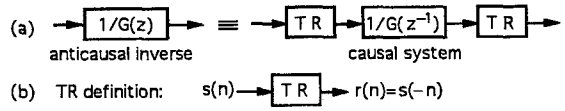

Fig. 1.2. The anticausal inverse represented in terms of a causal system and time-reversal operators.

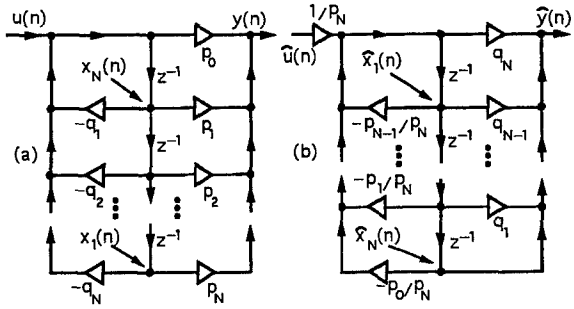

Fig. 2.1 (a) The direct-form structure, and (b) its causal dual.

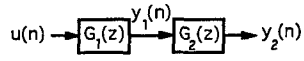

Fig. 2.2. A cascaded system.

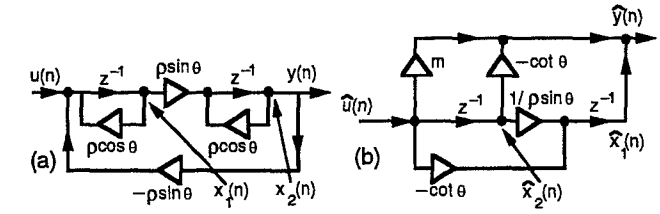

Fig. 3.1. (a) The coupled-form structure, and (b) its causal dual.

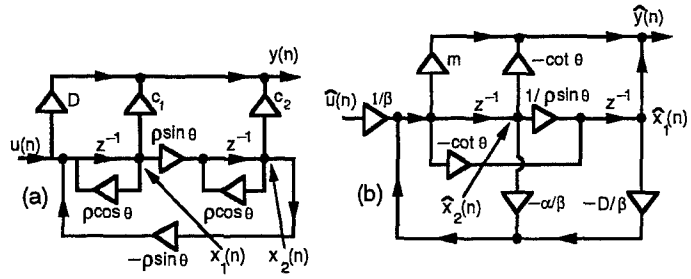

Fig. 3.2. (a) The tapped coupled form, and (b) its causal dual.

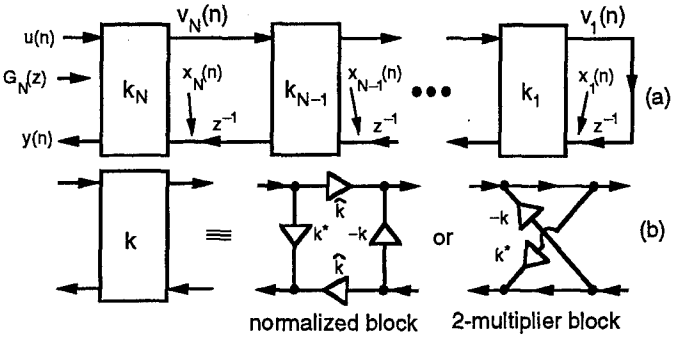

Fig. 4.1. (a) The general form of IIR allpass lattice, and (b) two possible building blocks.

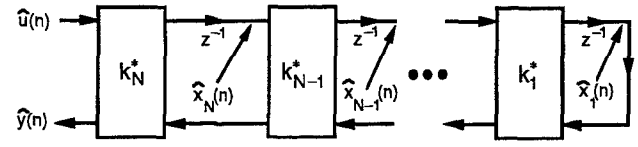

Fig. 4.2. The causal dual of the IIR lattice structure.

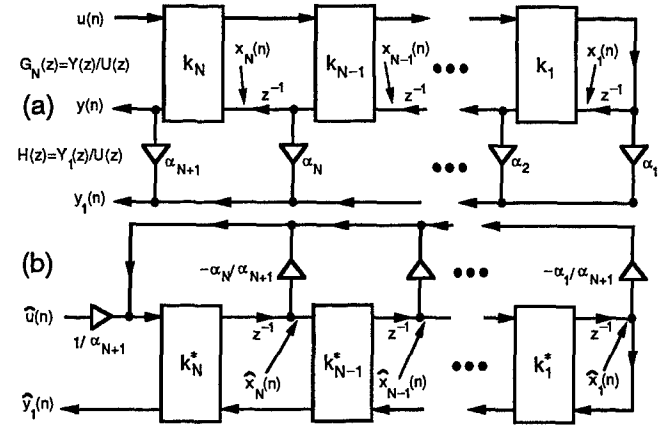

Fig. 4.3. (a) The tapped IIR lattice and (b) its causal dual.